PACS numbers: 442.79.Gn; 41.20.Jb
DOI: 10.1070/QE2005v035n02ABEH002639

Propagation of submillimetre laser beams in hollow waveguides

O.V. Gurin, A.V. Degtyarev, V.A. Maslov, V.A. Svich, V.M. Tkachenko, A.N. Topkov

***Abstract*. The mode and ray-optics techniques based on the representation of the input field as a spectrum of propagating modes or ray tubes are proposed for calculating the propagation of radiation in wide circular hollow waveguides excited by linearly polarised Gaussian beams. Optimal excitation conditions are determined theoretically and experimentally, and the degree of polarisation of the beams transmitted through the waveguides is evaluated.**

Keywords: *submillimetre laser, metal waveguide, dielectric waveguide, mode approach, ray-optics approach, excitation, polarisation.*

1. Introduction

Radiation beams formed in laser cavities and used for research and application purposes usually have a Gaussian intensity distribution in their cross section. Oversize hollow metal and dielectric waveguides are used for constructing resonators and transmission lines in the IR and submillimetre (SMM) wavelength ranges [1 – 3]. The designing of waveguide transmission lines requires information about energy losses in inhomogeneous radiation beams propagating in such systems, the conditions of their optimal excitation, the nature, magnitude and ways of minimising distortions introduced in the signals being transmitted.

The possibility of using waveguides with a diameter much larger than the wavelength as low-loss transmission lines was pointed out already in [4]. However, the propagation of SMM laser beams in waveguides has been studied extensively only in some recent theoretical and experimental works. Scattered information is available [5 – 9] about theoretical (using the geometrical optics technique) and experimental investigations of the coefficient of radiation transmission from gas-discharge lasers and optically pumped lasers (OPLs) through hollow waveguides. In [10], we studied the propagation of radiation in hollow dielectric waveguides excited by inhomogeneous radiation beams emerging from the central hole of the reflectors of a gas-discharge 337-μm HCN laser and a 118.8-μm OPL. OPLs can be tuned discretely over the entire SMM range from 0.1 to 1 mm and are more convenient for investigating the waveguide transmission of radiation.

The Marcatili – Schmeltzer relation $2\pi a/\lambda \gg |v|U_{kn}$ [11] describing the excitation in hybrid-mode waveguides, where a is the radius of the waveguide; v is the refractive index of the waveguide material; U_{kn} is the nth root of the equation $J_{k-1}(U_{kn}) = 0$ [J_{k-1} is the Bessel function of $(k-1)$th order]; and k and n characterise the propagating hybrid mode, is not satisfied for metal waveguides in the SMM range. For this reason, the metal waveguide parameters are calculated by the mode technique using analytic expressions for the waveguide TE and TM modes obtained in the 'ideal metal' approximation [12], although metals cannot be treated as ideal conductors in the short wavelength part of the SMM range. At the same time, dielectric waveguides are excited by strongly divergent radiation beams, when a considerable part of the energy is transferred by higher modes, for which the Marcatili – Schmeltzer approximation may not be satisfied either. Therefore, a verification of the mode approach in these cases requires the use of an alternative (e.g., ray-optics) method. The ray-optics techniques being used at present [7, 8] need to be developed further since they do not take into account the interference of beams incident on and reflected from the waveguide walls.

In this work, we have studied theoretically and experimentally the transmission of OPL radiation with a Gaussian intensity profile through hollow metal and dielectric waveguides to determine the optimal conditions for waveguide excitation, minimum depolarisation of the initial beam, and to work out recommendations for using these waveguides in SMM transmission lines.

2. Theoretical relations

2.1 Mode approach

Consider the excitation of a hollow circular metal waveguide by an axially symmetrical Gaussian beam polarised linearly in the direction y, whose field $\boldsymbol{E}_0 = \boldsymbol{y}_0 E_{0y}(x, y, 0)$ in the source plane $z' = 0$ has the form

$$E_{0y}(x,y,0) = \left(\frac{2}{\pi}\right)^{1/2} \frac{1}{\omega_0'} \exp\left(-\frac{x^2+y^2}{{\omega'}_0^2}\right), \qquad (1)$$

where $\boldsymbol{x}_0$ and $\boldsymbol{y}_0$ are the unit vectors of the Cartesian coordinates in the directions x and y, respectively; and ω_0' is the beam radius measured at the e^{-1} level of its maximum intensity.

O.V. Gurin, A.V. Degtyarev, V.A. Maslov, V.A. Svich, V.M. Tkachenko, A.N. Topkov V.N. Karazin Kharkov National University, pl. Svobody 4, 61077 Kharkov, Ukraine;
e-mail: Vyacheslav.A.Maslov@univer.kharkov.ua

Received 11 March 2004; revision received 15 September 2004
Kvantovaya Elektronika **35** (2) 175 – 179 (2005)
Translated by Ram Wadhwa

Let us pass to polar coordinates (r, φ) and introduce dimensionless parameters $\rho = r/a$, $\omega_0 = \omega_0'/a$. For the polarisation of the initial radiation beam specified in this manner, only the TE_{1n} and TM_{1n} waves will be excited in the waveguide [12], where the first subscript $m = 1$ is the azimuthal index, and the second subscript n is the radial index. The transverse electric field components for these waves were determined in [13]:

$$\boldsymbol{V}_{1n}^{\mathrm{TE}}(\rho, \varphi) = \boldsymbol{x}_0 A_{1n} J_2(\chi_{1n}\rho) \sin 2\varphi + \boldsymbol{y}_0 A_{1n} [J_0(\chi_{1n}\rho) - J_2(\chi_{1n}\rho) \cos 2\varphi],$$

$$\boldsymbol{V}_{1n}^{\mathrm{TM}}(\rho, \varphi) = -\boldsymbol{x}_0 B_{1n} J_2(\eta_{1n}\rho) \sin 2\varphi + \boldsymbol{y}_0 B_{1n} [J_0(\eta_{1n}\rho) + J_2(\eta_{1n}\rho) \cos 2\varphi],$$

where

$$A_{1n} = \frac{1}{J_2(\chi_{1n})\left[2\pi(\chi_{1n}^2 - 1)\right]^{1/2}}, \quad B_{1n} = \frac{1}{J_2(\eta_{1n})(2\pi)^{1/2}}$$

are the normalisation factors; J_j is the jth-order Bessel function of the first kind; χ_{1n} is the nth root of the equation $J_1'(\chi) = 0$; and η_{1n} is the nth root of the equation $J_1(\eta) = 0$.

In this case, the field distribution in the waveguide cross section at a distance z' from the entrance face of the waveguide has the form

$$\boldsymbol{E}(\rho, \varphi, z') = \sum_n C_n \boldsymbol{V}_{1n}^{\mathrm{TE}}(\rho, \varphi) \exp\left(\mathrm{i}\gamma_{1n}^{\mathrm{TE}} z'\right) + \sum_n D_n \boldsymbol{V}_{1n}^{\mathrm{TM}}(\rho, \varphi) \exp\left(\mathrm{i}\gamma_{1n}^{\mathrm{TM}} z'\right), \quad (2)$$

where the amplitudes C_n and D_n are defined by the relations

$$C_n = \iint \boldsymbol{E}_0 \boldsymbol{V}_{1n}^{\mathrm{TE}} \mathrm{d}S, \quad D_n = \iint \boldsymbol{E}_0 \boldsymbol{V}_{1n}^{\mathrm{TM}} \mathrm{d}S;$$

$\gamma_{1n} = \beta_{1n} + \mathrm{i}\alpha_{1n}$ are the propagation constants for the TE_{1n} and TM_{1n} modes [12].

By calculating the intensity of radiation $I(\rho, \varphi, z') = |E(\rho, \varphi, z')|^2$ at the point of observation, we determine the energy flux through the waveguide cross section at a distance z' from its entrance face:

$$W(z') = \int_0^{2\pi} \mathrm{d}\varphi \int_0^1 I(\rho, \varphi, z') \rho \mathrm{d}\rho. \quad (3)$$

The obtained relations allow us to determine the coefficient $T(z')$ of radiation transmission in the waveguide and the degree of polarisation $\Pi(z')$ of the output radiation:

$$T(z') = \frac{W(z')}{W(0)}, \quad \Pi(z') = \frac{I_y(z') - I_x(z')}{I_y(z') + I_x(z')}, \quad (4)$$

where

$$I_{x,y}(z') = \int_0^{2\pi} \mathrm{d}\varphi \int_0^1 \rho \mathrm{d}\rho |E_{x,y}(\rho, \varphi, z')|^2.$$

2.2 Ray-optics approach

Similarly to (1), we assume that the input beam is polarised along the y axis: $\boldsymbol{E}_0(\rho, 0) = \boldsymbol{y}_0 E_0(\rho, 0)$. Consider a Gaussian beam at a distance z' from the face of the waveguide. We introduce the normalised variable $z = z'/z_0$, where $z_0 = \pi\omega_0'^2/\lambda$ is the diffraction length of the beam. The field distribution of a Gaussian beam in the waveguide can be written in the form [14]

$$E(\rho, z) = \frac{(2/\pi)^{1/2}}{\omega_0(1 + z^2)^{1/2}} \exp\left[-\frac{\rho^2}{\omega_0^2(1 + z)}\right] \times \exp\left\{\mathrm{i}\left[\frac{\rho^2 z}{\omega_0^2(1 + z)} - \arctan z\right]\right\}.$$

We decompose the field vector of the propagating beam into two components – parallel and perpendicular to the plane of incidence on the waveguide wall:

$$\boldsymbol{E}(\rho, \varphi, z) = \boldsymbol{E}_{\|}(\rho, \varphi, z) + \boldsymbol{E}_{\perp}(\rho, \varphi, z),$$

where $E_{\|}(\rho, \varphi, z) = E(\rho, z) \sin \varphi$; and $E_{\perp}(\rho, \varphi, z) = E(\rho, z) \times \cos \varphi$.

By using geometrical optics, we assume that a beam consists of ray tubes or rays contained in an elementary solid angle, lying in the meridional planes of the waveguide and having a common origin – the centre of the beam. In such an analysis, it is not possible to determine the field at the axis of the waveguide [8]. At any other point of observation in the waveguide, the field is a superposition of the fields of the incident ray and the ray reflected from the waveguide wall. These rays can be assumed to emerge from the points displaced by $2k$ along ρ [8], where k is the number of reflections from the wall:

$$E_{\|}(\rho, \varphi, z) = \sum_k E_k(\rho_k, z) r_{\|}^{|k|} \sin \varphi,$$
$$E_{\perp}(\rho, \varphi, z) = \sum_k E_k(\rho_k, z) r_{\perp}^{|k|} \cos \varphi, \quad (5)$$

where $\rho_k = 2k + (-1)^k \rho$; $r_{\|}$ and $r_{\perp}$ are Fresnel's reflection coefficients [15].

The cross-sectional area that a ray tube would have possessed in the absence of reflections (Fig. 1) is $\mathrm{d}S_k = \zeta_k^2 \times \sin \Theta_k \mathrm{d}\varphi \mathrm{d}\Theta$ where

$$\Theta_k = \arctan \frac{\rho_k \lambda}{\pi \omega_0^2 a z};$$

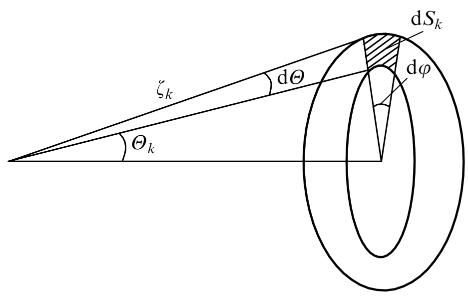

Figure 1. Cross section of a ray tube.

and $\zeta_k = z/\cos\Theta_k$ is the distance from the point of observation along the ray tube. We assume that a ray tube after reflection is focused into a line along the waveguide axis. In this case, the cross-sectional area of the ray tube at the point of observation is $dS = \zeta\sin\Theta d\varphi\zeta_k d\Theta$, where $\zeta = z/\cos\Theta$, and

$$\Theta = \arctan\frac{\rho\lambda}{\pi\omega_0^2 az}.$$

Because the energy flux in a ray tube is constant, the intensity $I_k'(\rho, z)$ at the given point is related to the intensity $I'(\rho_k, z)$ in the unfocused beam by the expression

$$I_k'(\rho, z) = \frac{dS_k}{dS} I'(\rho_k, z) = I'(\rho_k, z)\left|\frac{\rho_k}{\rho}\right|,$$

while the intensity of beams in the cross section perpendicular to the waveguide axis has the form $I_k(\rho, z) = I_k'(\rho, z)\cos\Theta_k$. Thus, the field of the kth beam in (5) is described by the expression

$$E_k(\rho_k, z) = E(\rho_k, z)\left(\left|\frac{\rho_k}{\rho}\right|\cos\Theta_k\right)^{1/2}.$$

By introducing the x- and y-components for the field in the left-hand side of (5), we derive the following expressions for them:

$$E_x(\rho, \varphi, z) = \frac{1}{|\rho|^{1/2}}\sum_k E(\rho_k, z)\left(r_{\parallel}^{|k|} - r_{\perp}^{|k|}\right) \times \sin\varphi\cos\varphi\,(|\rho_k|\cos\Theta_k)^{1/2},$$
$$E_y(\rho, \varphi, z) = \frac{1}{|\rho|^{1/2}}\sum_k E(\rho_k, z)\left(r_{\parallel}^{|k|}\sin^2\varphi + r_{\perp}^{|k|}\cos^2\varphi\right) \times(|\rho_k|\cos\Theta_k)^{1/2}. \quad (6)$$

The energy flux through the waveguide cross section in this approach is found from expression (3), while the coefficient of radiation transmission in the waveguide and the degree of polarisation of the output beam from expression (4).

3. Experimental setup

Figure 2 shows the scheme of the experimental setup. Gaussian beams with a plane wavefront are formed by an optical system consisting of spherical mirrors (*3*) with a radius of curvature $R = 50$ cm and mirrors (*5*) with different radii of curvature R. The divergent beam emerging from the SMM laser through the coupling hole of diameter 4 mm in the output mirror is incident on spherical mirror (*3*). The distance l_1 is chosen taking into account the beam divergence in such a way that a beam with a nearly plane phase front is formed in the plane of mirror (*5*). For the 118.8-μm radiation, the distance l_1 is 570 mm, while the distance l_2 between the spherical mirrors (*3*) and (*5*) is $l_2 = 1700$ mm. The beam diameters d at the level 1/10 of the maximum intensity at the entrance face of the waveguide obtained for different radii of curvature R of mirror (*5*) are presented in Table 1.

The beam diameters were measured by scanning with a pyroelectric detector in a plane perpendicular to the direction of the SMM radiation polarisation. The resolution of the detector used in experiments was 0.2 mm. In order to produce beams of diameter smaller than 2 mm, spherical mirror (*5*) was replaced by a plane mirror and Teflon lenses (*6*) of focal length 24, 14 and 9 cm were mounted at a distance of 24 cm from it. In this case, beams of diameter 1.7, 1.3 and 0.9 mm at the 1/10 level of maximum intensity were formed in the waist.

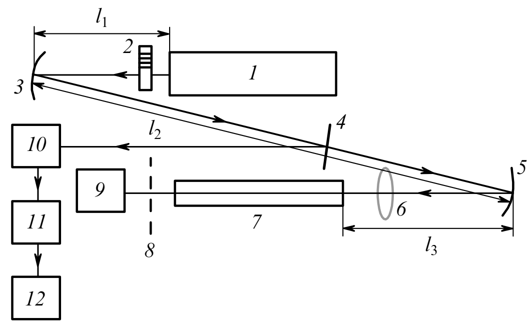

Figure 2. Scheme of the experimental setup: (*1*) SMM laser; (*2*) modulator; (*3*, *5*) spherical mirrors; (*4*) SMM radiation beamsplitter; (*6*) lens; (*7*) waveguide under study; (*8*) polariser; (*9*) power meter; (*10*) pyroelectric detector; (*11*) measuring amplifier; (*12*) oscillograph.

Table 1. Dependence of the beam diameter d on the radius of curvature R of a mirror.

R/cm	l_3/mm	d/mm
300	1160	6.5
200	875	5.1
100	475	3.5
50	240	2.2

The total attenuation δ_Σ (in dB m^{-1}) in the waveguide under study was calculated from the expression $\delta_\Sigma = (1/L)10\lg(P_0/P_1)$, where P_0 and P_1 are the radiation powers at the input and output of the waveguide, respectively; L is the waveguide length. The radiation powers P_0 and P_1 were measured with a BIMO-1 bolometer with a relative error of ±10 %. The attenuation of the 118.8-μm radiation was measured taking into account the atmospheric attenuation δ_{atm}, which was determined by measuring the power in two cross sections separated by a distance of ~ 1 m. The atmospheric attenuation depends on the humidity of air and is not a constant quantity. On different days, it varies in the range 0.5–0.7 dB m^{-1}. In this case, the attenuation in the waveguide is $\delta_w = \delta_\Sigma - \delta_{atm}$. The transmission coefficient T was calculated from the attenuation measurements.

The degree of polarisation of radiation was measured by mounting a one-dimensional wire grating polariser at the output of the waveguide. The degree of polarisation Π of the beam was calculated from the expression $\Pi = (P_\parallel - P_\perp)/(P_\parallel + P_\perp)$, where $P_\parallel$ and $P_\perp$ are the radiation powers for parallel and perpendicular arrangement of the grating relative to the direction of polarisation of the incident radiation.

4. Comparison of experimental and numerical results

The techniques described above were used for computer calculations and experimental measurements of the transmission coefficient and degree of polarisation of radiation in metal (copper) and dielectric (glass) waveguides excited by linearly polarised Gaussian beams from a 118.8-μm CH_3OH laser with a field of type (1). Investigations were performed by varying the relative radius ω_0 of the initial beam in the range 0.1 – 0.9 (in its 'weak' diffraction region [16]). The surface resistance of copper taking into account the dc conductivity of the metal $\sigma_0 = 5.73 \times 10^7$ S m^{-1} is $R_s = 2.625 \times 10^{-7}(c/\lambda)^{1/2}$ [17]. According to [18], at $\lambda = 118.8$ μm, the theoretical value of the refractive index is $\nu \approx 216 + i576$. The transmission coefficient of the dielectric waveguide was calculated using the mode technique described by us in [19]. Pyrex glass with a theoretical refractive index $\nu \approx 2.32 + i0.40$ at $\lambda = 118.8$ μm was chosen as the material for this waveguide [20].

Figure 3 shows the results of measurements and calculations of transmission parameters of copper and glass waveguides of identical geometrical dimensions: diameter $2a = 5.7$ mm ($a/\lambda \approx 24$) and length $L = 60$ mm. Such a choice of the waveguide length was dictated by the restriction imposed on this parameter in the ray-optics approach and by the need to perform calculations for $L < a^2/\lambda$ [8]. The results presented in the figure demonstrate qualitative agreement between the experimental and theoretical data obtained by using various techniques. This justifies the use of mode approach in the ideal metal approximation at wavelengths exceeding 0.1 mm, and this technique was employed in subsequent calculations.

We studied experimentally and theoretically copper waveguides of different sizes with parameters $2a = 5.7$ mm ($a/\lambda \approx 24$), $L = 500$ mm and $2a = 7.8$ mm ($a/\lambda \approx 33$) and length $L = 400$ mm, as well as glass waveguides with parameters $2a = 5.7$ mm ($a/\lambda \approx 24$), $L = 500$ mm and $2a = 8.5$ mm ($a/\lambda \approx 36$), $L = 500$ mm. Figure 4 shows the results of investigation of the transmission coefficient and the degree of polarisation of the output radiation from these waveguides. One can see that unlike dielectric waveguides, the metal waveguides have a transmission coefficient that varies weakly with changing the exciting beam radius and does not have an optimal value. An analysis of the results of calculations by the mode technique shows that for small values of ω_0, the main part of the exciting beam energy is transferred by the higher-order modes that have a weaker attenuation. As the value of ω_0 increases, the key role in the emission spectrum is played by the TE_{11} and TM_{11} modes with a stronger attenuation than other modes, which explains a decrease in the transmission coefficient for metal waveguides in the case of broad exciting beams. Dielectric waveguides are characterised by a pronounced optimal value of the maximum coefficient of radiation transmission in a waveguide corresponding to the range $0.5 < \omega_0 < 0.7$, which well agrees with the analogous results obtained during the transmission of single-mode and multimode radiation [5, 7, 8, 21 – 24]. This optimum corresponds to the transfer of the highest fraction of the exciting beam energy to the fundamental EH_{11} mode of the dielectric waveguide, which has the lowest attenuation [11].

The degree of polarisation of the transmitted radiation in dielectric waveguides is close to 100 % and is preserved quite well over the entire range of variation of the parameters of the beams under study. In metal waveguides, the degree of polarisation of the output radiation increases

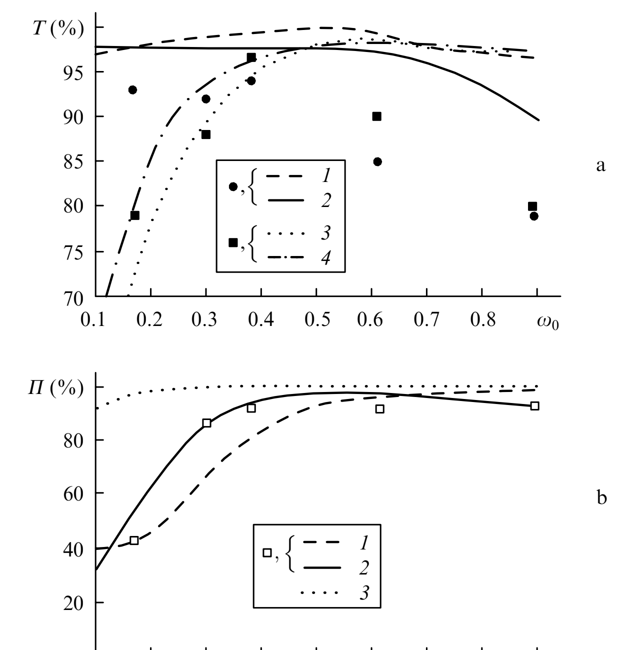

Figure 3. Calculated (curves) and experimental (dots) dependences of (a) the transmission coefficient T and (b) the degree of polarisation Π of radiation on the relative radius ω_0 of the exciting beam in a metal (*1*, *2*) and dielectric (*3*, *4*) waveguides for $2a = 5.7$ mm, $L = 60$ mm. Curves (*1*, *3*) were calculated by using the ray-optics technique, while curves (*2*, *4*) were obtained by employing the mode technique.

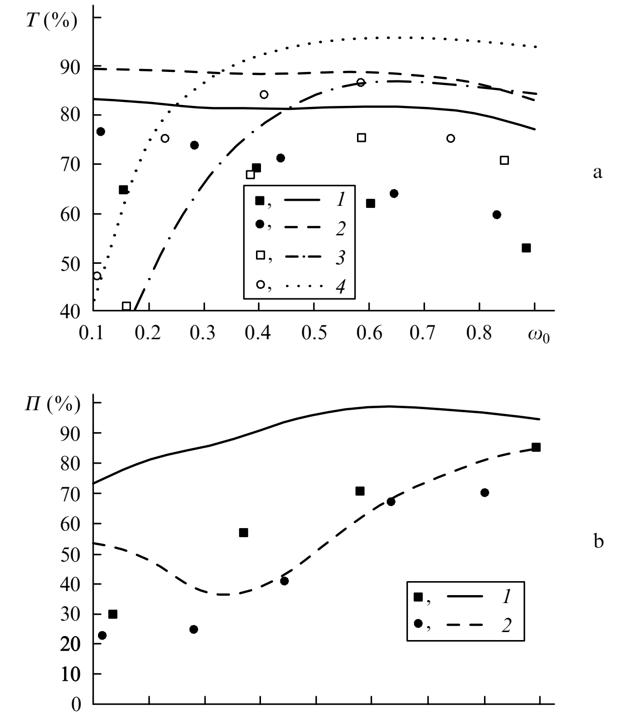

Figure 4. Calculated (curves) and experimental (dots) dependences of (a) the transmission coefficient T and (b) the degree of polarisation Π of radiation on the relative radius ω_0 of the exciting beam in a metal (*1*, *2*) and dielectric (*3*, *4*) waveguides for $2a = 5.7$ mm, $L = 500$ mm [curve (*1*)], $2a = 7.8$ mm, $L = 400$ mm [curve (*2*)], $2a = 5.7$ mm, $L = 500$ mm [curve (*3*)] and $2a = 8.5$ mm, $L = 500$ mm [curve (*4*)].

with increasing exciting beam radius and with decreasing a/λ, which is explained by the increase in the contribution from the TE_{11} guided mode (with the highest fraction of linearly polarised radiation among all modes) to the radiation spectrum.

The difference between the experimental and theoretical data is due to the irregularities in the cross section, roughness of the surface and the possible difference in the theoretical material constants for the waveguides used in the study.

5. Conclusions

We have studied theoretically and experimentally the propagation of linearly polarised Gaussian beams of SMM laser radiation in hollow metal and dielectric circular waveguides. New mode and ray-optics approaches for calculating the transmission parameters of radiation in waveguide transmission lines have been proposed on the basis of the input field presentation as a spectrum of propagating modes or ray tubes lying in the meridional planes of the waveguide and intersecting only at its axis, and taking into account the interference of the beams incident on and reflected from the waveguide walls.

Conditions for optimal excitation of hollow circular waveguides excited by inhomogeneous Gaussian radiation beams with a plane phase front at the waveguide input have been studied. It is found that for dielectric waveguides, the highest transmission coefficient is achieved when the ratio of the beam radius to the radius of the waveguide is equal to 0.5 – 0.7. Metal waveguides are preferable transmission lines for the SMM radiation in the case when the radius of the exciting beam does not exceed ~ 0.3 of the waveguide radius.

The degree of polarisation of the transmitted radiation is close to 100 % for dielectric waveguides and is preserved over the entire range of variation of parameters of the beams under study. Metal waveguides are characterised by an increase in the degree of polarisation of the output radiation with increasing the exciting radiation beam radius and decreasing the waveguide radius.

References

1. Meriakri V.V. *Zarubezhn. Radioelektron. Usp. Sovr. Radioelektron.*, (12), 1 (2002).
2. Kneubuhl F.K., Alfolter E., in *Infrared and Millimeter Waves* (New York: Acad. Press, 1979) Vol. 1, p. 235.
3. Roser H.P., Yamanaka M., Wattenbach R., Schultz G.V. *Int. J. Infrared & Millimeter Waves*, **3**, 839 (1982).
4. Kapitza P.L., in *Elektronika bol'shikh moshchnostei* (High-power Electronics) (Moscow: Izd. Akad. Nauk SSSR, 1962).
5. Crenn J.P. *IEEE Trans. Microwave Theory and Techn.*, **27**, 573 (1979).
6. Crenn J.P., Veron D. *Proc. VI Int. Conf. Infrared and Millimeter Waves* (Miami Beach, USA, 1981) p. 189.
7. Crenn J.P. *Appl. Opt.*, **21**, 4533 (1982); **24**, 3648 (1985).
8. Frost B.S., Gourlay P.M., Heckenberg N.R., et al. *Appl. Opt.*, **24**, 4414 (1985).
9. Ensheng F. *J. Opt. Soc. Am. B*, **13**, 702 (1996).
10. Epishin V.A., Maslov V.A., Ryabikh V.N., et al. *Kvantovaya Elektron.*, **17**, 480 (1990) [*Sov. J Quantum Electron.*, **20**, 415 (1990)].
11. Marcatili E.A.J., Schmeltzer R.A. *Bell. Syst. Techn. J.*, **43**, 1783 (1964).
12. Fel'd Ya.N. (Ed.) *Spravochnik po volnovodam* (Handbook on Waveguides) (Moscow: Sov. Radio, 1952).
13. Gurin O.V., Degtyarev A.V., Maslov V.A., et al. *Kvantovaya Elektron.*, **31**, 346 (2001) [*Quantum Elektron.*, **31**, 346 (2001)].
14. Tarasov L.V. *Fizika protsessov v generatorakh kogerentnogo opticheskogo izlucheniya* (Laser Physics) (Moscow: Radio i Svyaz', 1981).
15. Born M., Wolf E. *Principles of Optics* (Oxford: Pergamon Press, 1969; Moscow: Nauka, 1973).
16. Belland P., Crenn J.P. *Appl. Opt.*, **21**, 522 (1982).
17. Tisher F.J. *Proc. VIII Eur. Microwave Conf.* (Paris: Sevenoaks, 1978) p. 524.
18. Ordal M.A., Bell R.J., Alexander R.W., et al. *Appl. Opt.*, **24**, 4414 (1985).
19. Epishin V.A., Maslov V.A., Ryabikh V.N., et al. *Radiotekhn. Elektron.*, **33**, 700 (1988).
20. Birch J.R., Cook R.J., Harding A.F., et al. *J. Phys. D: Appl. Phys.*, **8**, 1353 (1975).
21. Zyatitskii V.A., Kazantsev Yu.N. *Izv. Vyssh. Uchebn. Zaved. Ser. Radiofiz.*, **14**, 1570 (1971).
22. Abrams R.L. *IEEE J. Quantum Electron.*, **8**, 838 (1972).
23. Pasquet D., Gautier J.L., Pouvil P. *Int. J. Infrared & Millimeter Waves*, **9**, 555 (1988).
24. Belland P., Crenn J.P. *Int. J. Infrared & Millimeter Waves*, **10**, 1279 (1989).